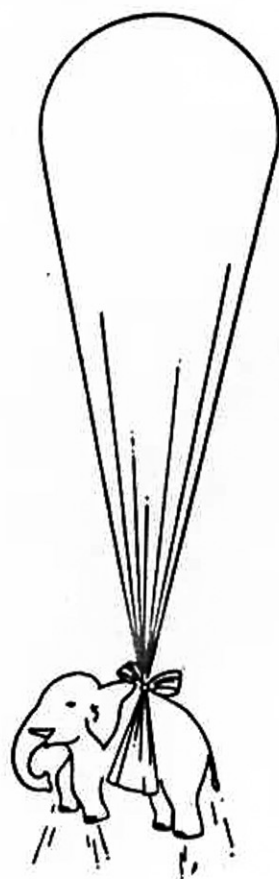


# 18TH INTERNATIONAL COSMIC RAY CONFERENCE

BANGALORE, INDIA-AUGUST 22 TO SEPTEMBER 3, 1983

## LATE PAPERS

**MG**  
**SP**  
SESSIONS  
VOL. 10



SOLAR PARTICLE CORROTATING EVENTS FROM SHOCKED NEUTRAL SHEETS  
D J MULLAN, Bartol Research Foundation, Newark, Delaware 19711  
J. PEREZ-PERAZA, M GALVEZ, M ALVAREZ, Instituto de Geofisica,  
UNAM, 04510, Mexico D.F.

## 1. INTRODUCTION

In this work, we consider a process for prolonged particle acceleration. This process involves the interaction between a shock and a particular magnetic structure in the corona, namely a neutral sheet, such as that which is associated with a Helmet-Streamer. This interaction has already been considered in a different context by Steinolfson and Mullan (1980). In that work, the primary interest was to study what effect the neutral sheet had on the shock. Here we ask the opposite question: what effect does the shock have on the neutral sheet? Because the shock deposited some of its energy, the net effect of shock passage is to cause the neutral sheet to be compressed. The increase in plasma temperature leads to a decrease in the conductivity of the plasma. Magnetic diffusion is enhanced causing the sheet to collapse more rapidly. The accompanying increase in electric field in the sheet enhances the efficiency of particle acceleration. Hence, in the cases of flare shocks that collide with Helmet-Streamers, their neutral sheet can act as a delayed prolonged source of energetic particles after a flare. To test this proposal of Mullan (1979) some features of the acceleration process need to be evaluated.

## 2. ACCELERATION IN SHOCKED NEUTRAL SHEETS

In the work of Steinolfson and Mullan, the neutral layer was simulated initially as a vertical structure extending radially from the solar surface (fig. 1). At the time  $t=0$ , the flare was simulated by a pressure pulse off to one side of the neutral sheet. As the shock expands, the neutral sheet is pushed away from its original position (fig. 2). Around the neutral sheet, there exists a so-called diffusion region, which is the volume of acceleration of interest to us here. In order to delineate the boundaries of the diffusion region we followed the next criteria: the shock enhancement of gas pressure is greatest in the vicinity of the neutral sheet. So in Figs. 3 and 4 it is shown the evolution of the distribution of pressure. It can be seen that there is a well-defined ridge of high pressure, showing where shock processing has been strongest. We choose the cut-off contour where the pressure has increased by a factor of 3.5 relative to the initial ambient pressure (fig. 5). Since the diffusion region will occur at points where the magnetic Reynolds number fall to a relatively low value, we evaluated the magnetic Reynolds number ( $R_{\eta}$ ) at each point of the computational grid and we found similar dimensions for the diffusion region (fig. 6). As a first approximation to calculate neutral sheet acceleration, we consider an analytic formulation (Pérez-Peraza, et al, 1977) where the energy spectrum of particles is obtained.



after solving the motion equations of particles within the specific topology of the shocked neutral sheet. The method requires of the neglect of the drift velocities in the z-coordinate where the induced electric field is directed. The analytic magnetic topology was constructed from the discrete data of the previously mentioned simulation by transforming the polar coordinates to a cartesian system. We obtained a configuration of the form  $B=(B_x, B_y, 0)$  with  $B_x=B_0PY$ ,  $B_y=B_0KX$  and  $B_0=3.1977$  gauss, where  $P=21$  and  $K=0.7$ . If we can assume a large scale uniformity of the electric field, for a given magnetic field topology the maximum cut-off energy of the particle spectrum depends on the electric field according to  $E^{4/3}$ . Hence, if we can characterize the neutral sheet by one particular value of the electric field strength, the spectrum of particles which will emerge is predictable by the expression given in the work of Pérez-Peraza et al, with a cut-off when the energy reach the value  $\epsilon_0=(q^2mc^2/B_0^2P^2)^{1/3} E^{4/3}$ . In figs.7 and 8 we show the spectral fits which we have obtained to some delayed events. The free parameter in obtaining the fits with the data is the field  $E$ ;  $Q$  and  $N$  are the flux and energy of normalization respectively. Now in order to overcome the simplification of an overall value of  $E$  and the neglect of drift velocities, the spectrum was also derived numerically by following individual particle trajectories. We developed a 'Box-Wise' analysis across the diffusion region, composed of 112 boxes of the grid which was used in the ideal MHD simulation (fig.10). The electric field varies from point to point because the discrete values of the magnetic field from the simulation are fitted to a continuous topology. So the method is based in solving in heliocentric cartesian coordinates the complete motion equations, holding constant the magnetic field, during fractions of gyro period. Results are stabilized for evaluations every 0.05 of gyro-period. This is the way as particles feel the magnetic field structure. For the electric field evaluations, the diffusion velocities in each box were calculated as the relative velocity between the borders of the sheet and matter in the boxes by subtracting the velocity of the N.L. With the former convention,  $V_d < 0$  in the section  $B^+$  and  $V_d > 0$  in the sector  $B^-$  implies classical magnetic diffusion (designed here as compression) in the sense that the resultant motion is towards the N.L., whereas  $V_d > 0$  in the sector  $B^+$  and  $V_d < 0$  in the sector  $B^-$  entails a 'no-classical' kind of shocked-magnetic diffusion (designated here as relaxation), because the resultant motion is opposite to the N.L. On fig.10 compression and relaxation areas correspond to black and white boxes respectively. Assuming that all particles in a box, of a given density, reach the same energy, we are able to build the differential spectrum (fig.9). The encircled crosses give the spectrum built smoothing the fluxes by energy bands. The law  $E^{-0.48}$  is in agreement with what is expected in the vicinity of the source of delayed events (fig.6 in Christon, 1981).

DISCUSSIONS AND CONCLUSIONS : The required values of the constant  $E$ , by the analytical method ( $10^{-4}$ - $10^{-3}$  c.g.s. units) overlap



significantly with the range of values which were found in the shock simulation of Steinolfson and Mullan. There is in principle no reason whatever to expect that the range of  $E$  turn out to be what is needed to explain the observed spectra. This leads us to suspect that the observed particle spectra are consistent with acceleration in coronal shocked neutral sheets. Also, in spite of the approximation made in the analytic analysis, from the consistence with the numerical approach in predicting values of  $\epsilon_0 = 1-100$  MeV, it turns to be a high efficient method to calculate particle spectra. Fig.10 illustrates typical trajectories, where their history is easily understood in terms of the relative importance between the electric field  $(V_p \times B)/c = E_p$  and  $E$  in the Lorentz accelerating force. Trajectories may be coupled in 4 groups: particles whose trajectories remain in sectors of  $F$  minimum (I), of maximum force (II), particles going from sectors of  $F$  maximum to  $F$  minimum (III) and particles going from sectors of  $F$  minimum to  $F$  maximum (IV). Each one of these modalities, with acceleration or deceleration depending on the combinations of the orientations of  $B$  and  $\theta$ . This will be discussed elsewhere in detail.

REFERENCES: Christon, S.P., 1981, J.G.R., 86, 8852  
 Kinsey, J.H., 1970, Phys.Rev.Lett., 24, 246.  
 Lanzerotti, D.J., 1969, J.G.R., 74, 2851.  
 Mullan, D.J., 1979, AIP Conf. Proc. No.56  
 Pérez-Peraza J., Galvez, M. and Lara, R., 1977, Proc. 15ICRC, 5, 23  
 Steinolfson, R.S. and Mullan, D.J., 1980, 241, 1186.

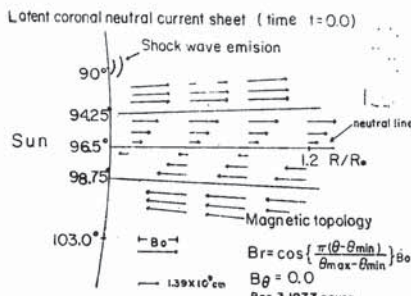


Fig. 1

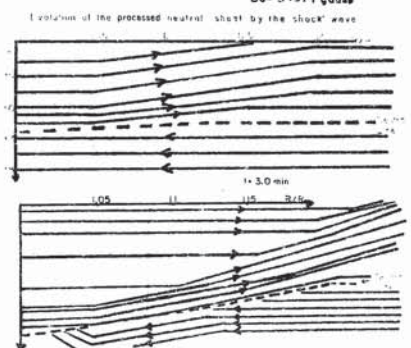


Fig. 2

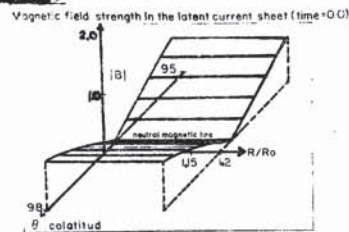


Fig. 3

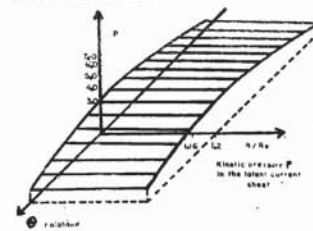


Fig. 6

